

Enhanced transmission due to nonplasmon resonances in one- and two-dimensional gratings

Evgeny Popov, Stefan Enoch, Gérard Tayeb, Michel Nevière, Boris Gralak, and Nicolas Bonod

Enhanced transmission through subwavelength slit gratings and hole arrays is studied in view of its application in the far-infrared and microwave domains. Because for perfectly conducting gratings, plasmon resonances are not expected to produce an enhanced transmission, other kinds of resonance, such as Fabry–Perot, waveguide-mode, and cavity-mode resonances, are studied. The possibility of reaching 100% transmittivity for some particular wavelengths is established when two superimposed identical gratings are used while each of them transmits approximately 1% off resonance. A similar transmission is obtained with hole arrays. The study of the field map inside the groove region allows our establishing the nature of the resonance, that is involved. Comparison of the bandwidth with respect to the wavelength or incidence given by various kinds of resonance is presented. © 2004 Optical Society of America

OCIS codes: 050.1950, 050.0050, 050.2230.

1. Introduction

Since the famous study of R. Wood,¹ it is well known that electromagnetic effects can play a key role in the diffraction behavior of gratings. Fano² was the first to propose that some anomalies could be explained by surface waves (nowadays called plasmons) along the metallic–dielectric interface. Similar effects are observed when guided waves propagate along dielectric waveguides. Corrugated waveguides have been extensively studied since the 1970's as grating couplers in integrated optics.³ Later, they gave rise to the domain called, in the 1990's, subwavelength gratings, characterized by the fact that only the specular orders can propagate in the cladding and the substrate.⁴ These gratings have a remarkable property to have reflection and transmission growing from 0%

to 100% within a fraction of the incident wavelength or angle-of-incidence variation.

In 1997, Ebbesen *et al.*⁵ observed an enhanced transmission through a metallic film pierced with periodically arranged holes. Although the holes introduce a channel for light propagation more efficient than the simple tunneling through the continuous film,⁶ the enhanced transmission is predominantly due to the plasmon excitation on one or both film surfaces, so that the effect could also be observed at corrugated surfaces having a constant thickness.⁷ It is necessary to point out that hole arrays significantly differ from slots (or grid gratings) because the latter can support a TEM mode that propagates with small decay through the grating thickness, whereas the former cannot support it. The existence of this TEM mode explains the drastic difference in behavior between TE- (electric field vector parallel to the slit direction) and TM-polarized light diffraction by metallic grids. Whereas TM-polarized light is easily transmitted, TE-polarized light is reflected backward, thus the use of such gratings as grid polarizers.^{8–10} Hole arrays provide a mixed response because the TEM mode does not exist, and, for subwavelength periods, all the modes inside the hollow (hole) guide are evanescent. Thus the nonresonant (background) transmission is relatively low and is significantly enhanced only in the spectral and angular regions in which surface plasmons are excited along the metallic surface. This excitation be-

E. Popov (e.popov@fresnel.fr), S. Enoch, G. Tayeb, M. Nevière, and N. Bonod are with the Institut Fresnel, Unité Mixte de Recherche associée au Centre National de Recherche Scientifique 6133, Faculté des Sciences et Techniques de Saint-Jérôme, Case 161, Avenue Escadrille Normandie Niemen; 13397 Marseille Cedex 20, France. B. Gralak is with the Institute for Atomic and Molecular Physics, Foundation for Fundamental Matter, Kruislaan 407, 1098 SJ, Amsterdam, The Netherlands.

Received 7 May 2003; revised manuscript received 15 September 2003; accepted 28 October 2003.

0003-6935/04/050999-10\$15.00/0

© 2004 Optical Society of America

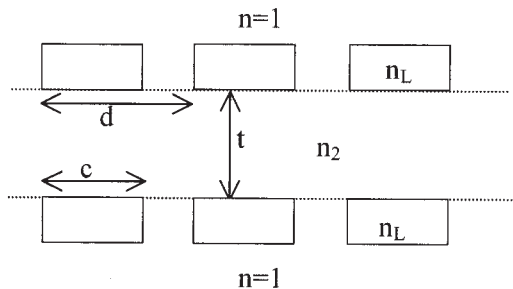


Fig. 1. Schematic representation of a double-grating structure consisting of two identical grid gratings.

comes possible owing to the grating periodicity (one-dimensional or two-dimensional), which adds one or more grating vectors to the wave-vector component parallel to the grating surface.

A discussion has recently arisen¹¹ concerning the existence of enhanced transmission in metallic gratings having (almost) infinite conductivity, similar to the effect observed by Ebbesen. Whereas for a one-dimensional grating the fundamental TEM mode ensures enough transmission in TM polarization even without plasmon effects,¹² for hole arrays or crossed grids, resonances are necessary to enhance the otherwise too-weak transmission. However, plasmons along the subwavelength almost perfectly conducting gratings working in specular order cannot produce visible effects in the reflectivity.¹³ To observe their effect, it is necessary to introduce losses, absorption or diffraction.¹¹ However, losses in most cases are not desirable. Thus the natural question that arises is whether it is possible to use other types of electromagnetic resonance, rather than the surface-polariton-plasmon excitation, to obtain enhanced transmission in perfectly conducting crossed grids or hole-array gratings. Another question concerns the intensity of the enhancement in TE polarization for one-dimensional gratings.

Our aim in this paper is to analyze the role of other known resonance phenomena for the transmission enhancement in otherwise weakly transmitting gratings. These will be the Fabry–Perot resonances, the waveguide-mode excitation, and the cavity modes. In some cases it will be difficult to distinguish among these three phenomena, owing to their gradual mutation from one into another. To determine which is which, we study the electric field map distribution inside the grating structure. The possibility of obtaining enhanced transmission by use of a double-grating structure has been known for quite a long time.¹⁴ In fact, the basic principle of Fabry–Perot resonances lies in the possibility to constructively interfere light transmitted and reflected by two consecutive structures. Provided that symmetry with respect to a horizontal plane (Fig. 1) is fulfilled, one can expect a 100% maximum of transmission¹⁵ of the two combined gratings, even if the transmission of each of them is quite small. Thus, if a single grating transmits less than 1%, adding an identical structure not only does not always diminish the transmission

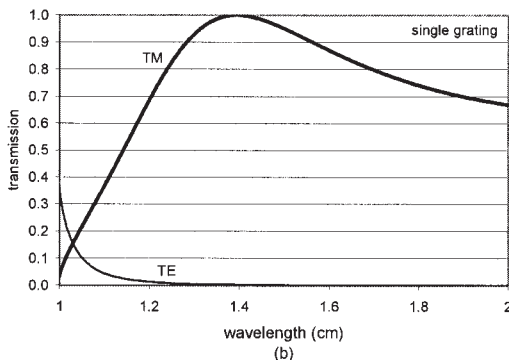
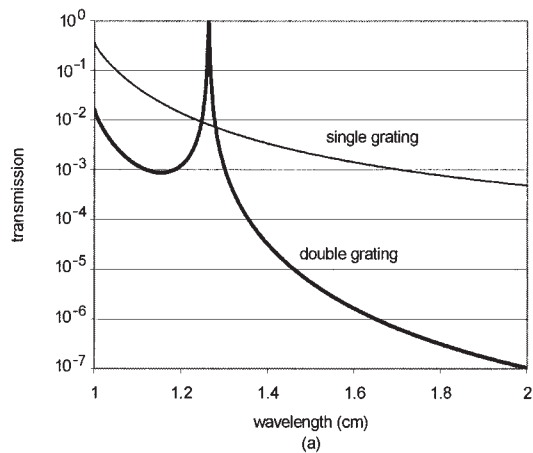


Fig. 2. (a) Transmission through a single or a double-grating structure. $d = 1$, $c = 0.5$, $t = 0.5$, lamellae thickness is 0.5, and refractive index $n_L = i250$; all units are in centimeters. (b) Transmission through a single grating in TE or TM polarization [same parameters as in (a)].

100 times more, but, at a given distance or for a particular wavelength, it increases it to 100% [Fig. 2(a)]. As already discussed, owing to the existence of surface plasmon resonance, even a single-grating structure could totally transmit TM polarization [Fig. 2(b)]. To eliminate the possible (if any) influence of plasmon surface waves, we first deal with a one-dimensional grating structure in TE polarization, for which plasmons cannot propagate. Next we go to two-dimensional structures and are able to obtain similar behavior.

2. One-Dimensional Grating in TE Polarization

At first, we consider a structure that will be called a grating–waveguide configuration [Fig. 3(a)]. This is a one-dimensional lamellar grating consisting of two rows of metallic slits situated at the two faces of a continuous dielectric film with refractive index $n_2 = 3.47$. The outermost media have refractive index $n = 1$. In what follows we assume a TE-polarized (electric field parallel to the grooves) plane monochro-

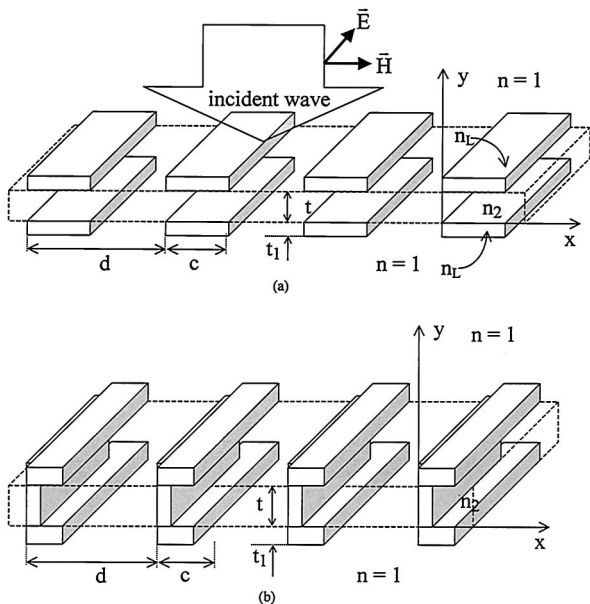


Fig. 3. Schematic representation of two types of a one-dimensional slit grating: (a) a double grating with a continuous dielectric layer in the middle, called the grating-waveguide configuration, and (b) a grating-cavity configuration.

matic wave under normal incidence with respect to the grating plane. The wavelength is $\lambda = 1.5$ cm, and the period is $d = 1$ cm, so that only the specular orders propagate in the cladding and the substrate.

As already discussed at the end of Section 1, a single-row slit grating has a quite weak transmission under the chosen conditions. Adding a second row introduces interference phenomena that could lead to almost total transmission at some set of optogeometrical parameters of the system. Figure 4 represents the transmission of the grating of Fig. 3(a) as a function of the slit width c and the middle-layer thickness t . The lamellae thickness is $t_1 = 0.1$ cm. Lamellae are taken to be lossless with the optical index equal to $n_L = i250$. The calculations are made by use of the rigorous coupled-wave method¹⁶ and confirmed in the limit of perfectly conducting lossless

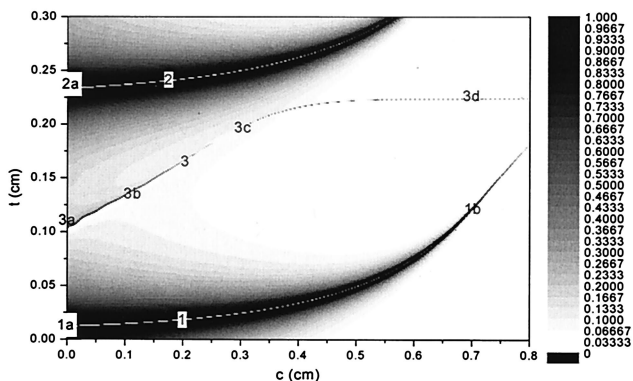


Fig. 4. Transmission as a function of the lamellae width (c) and middle-layer thickness (t) in centimeters for the grating represented in Fig. 3(a).

material by use of the rigorous modal method.¹⁷ As $n_L \rightarrow i\infty$, the system response varies insignificantly, provided that the lamellae dimensions are large enough so that their optical thickness could be considered much larger than the wavelength. This is not the case when the lamellae are too thin.¹⁸ For that reason, we will draw the curves for $c > 0.1$ for Fig. 3(b). On the other hand, when $c \rightarrow d$, the resonances become too thin to be observed; thus we will limit the range of c to $c < 0.8$.

Although the overall background values of transmission are quite low, there are three distinct regions in which the transmission reaches 100%. The three curves are numbered from 1 to 3 in the figure. Regions 1 and 2 are wider for thinner lamellae (c small). Let us study in more detail the limit when the lamellae width tends toward the period, $c \rightarrow d$; i.e., the resonator is completely closed. We recall that, when the m th mode of a slab is excited in TE polarization through the p th order of the grating, we obtain the well-known formula

$$\left(\frac{2\pi n_2}{\lambda}\right)^2 - \left(\frac{p2\pi}{d}\right)^2 = \left(\frac{m\pi}{t}\right)^2. \quad (1)$$

The thicknesses corresponding to 100% transmission then tend to the following values:

curve 1: $t \rightarrow 0.216$ cm such that

$$\frac{2\pi}{\lambda} n_2 t = \pi, \quad (2)$$

curve 2: $t \rightarrow 0.432$ cm such that

$$\frac{2\pi}{\lambda} n_2 t = 2\pi, \quad (3)$$

curve 3: $t \rightarrow 0.240$ cm such that

$$\frac{2\pi}{\lambda} \left[n_2^2 - \left(\frac{\lambda}{d}\right)^2 \right]^{1/2} t = \pi. \quad (4)$$

The first two thickness values correspond to the first two waveguide modes of the hollow metallic waveguide made of metallic plates surrounding the dielectric layer. The third thickness corresponds to the first waveguide mode excited through the first grating order propagating inside the dielectric layer.

The other limit $c \rightarrow 0$ corresponds to a completely open dielectric waveguide without metallic lamellae. As already said, this limit has to be numerically taken rather carefully¹⁸; it is important to have the limit $n_L c \rightarrow 0$ fulfilled. In that limit, the thicknesses corresponding to curves 1 and 2 tend toward the values giving the Fabry-Perot resonances for a bare dielectric layer (curve 1 tends toward zero thickness, which corresponds to 100% transmission), whereas the resonance thickness of the third curve tends toward the value 0.052 cm, which provides excitation of the fundamental mode of the corresponding dielectric waveguide through the first diffraction order. Table

Table 1. Values of the Resonant Thickness of the Dielectric Layer Corresponding to Curve 3 of Fig. 4 When $n_L c \rightarrow 0$

n_L	$\text{abs}(n_L c)$	Resonant Thickness t (cm)
$0 + i250$	5	0.1072
$0 + i100$	2	0.1065
$0 + i50$	1	0.1037
$0 + i20$	0.4	0.0943
$0 + i10$	0.2	0.0786
$0 + i5$	0.1	0.0628
$0 + i2$	0.04	0.0547
$1 + i0$	0.02	0.0526

1 presents the change of the resonance thickness t corresponding to point 3a of Fig. 4, when the imaginary part of n_L gradually tends toward zero, keeping c constant. As one can observe, the value of t tends toward 0.052.

To better illustrate the similarities and the differences between the different curves, we present the distribution of the electric field inside the grating region for several characteristic points along the different curves in Fig. 4. Figures 5(a)–5(c) give the electric field (E_z) for the three points 1a, 2a, and 1b, respectively. The modulus of the incident electric

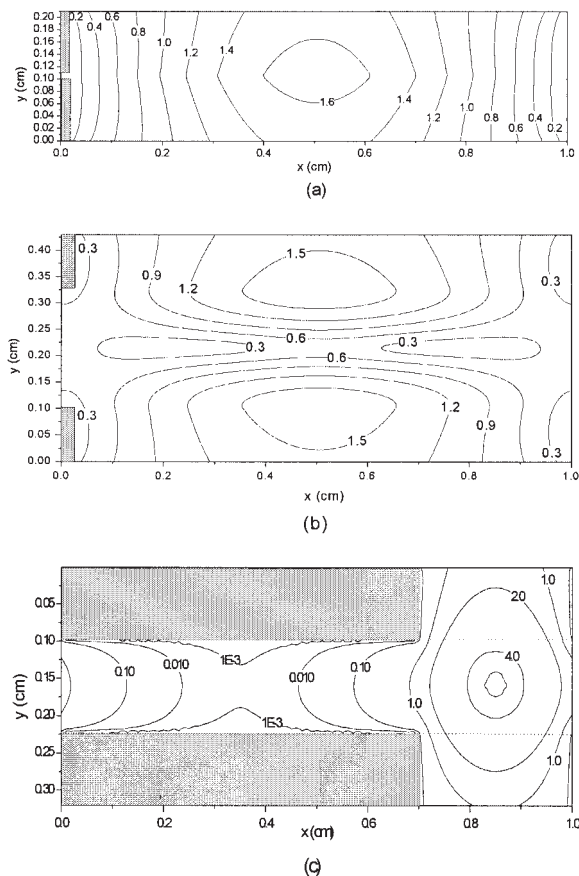


Fig. 5. Electric field maps corresponding to different working points of Fig. 4: (a) point 1a with $c = 0.02$, (b) point 2a with $c = 0.2$, and (c) point 1b with $c = 0.7$.

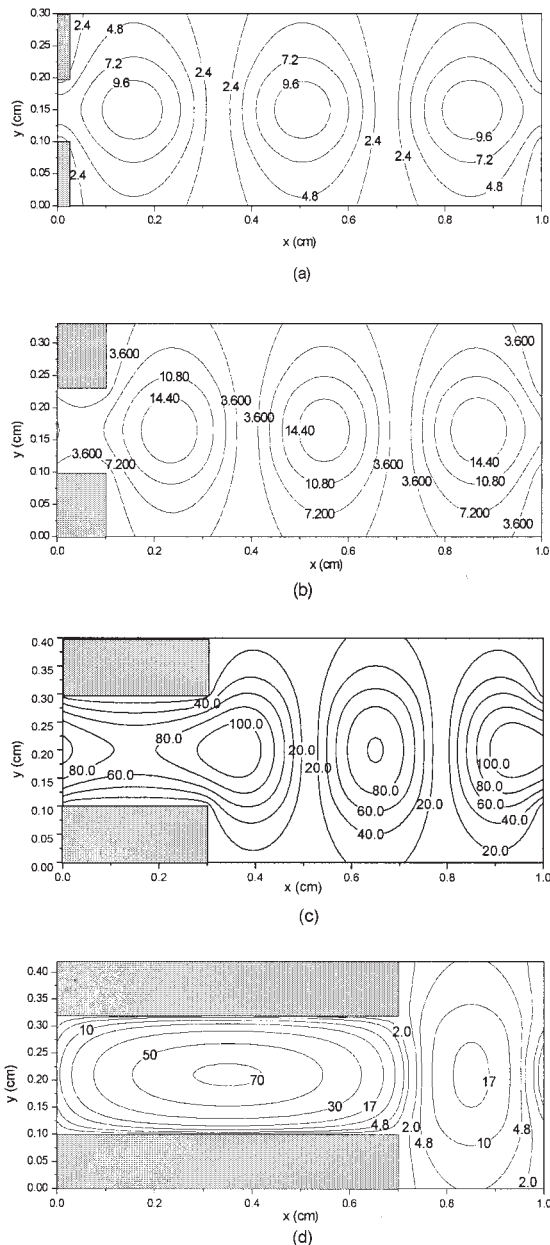


Fig. 6. Electric field maps corresponding to different working points along curve 3 of Fig. 4: (a) point 3a with $c = 0.02$, (b) point 3b with $c = 0.1$, (c) point 3c with $c = 0.3$, and (d) point 3d with $c = 0.7$.

field is taken equal to 1. At points 1a and 2a, the field is weakly depending on the x coordinate and presents a single (for point 1a) or a double (for point 2a) resonance in the y direction. This behavior is typical of the Fabry–Perot resonances, which are completely x independent when $c = 0$. Going to the right-hand side of Fig. 4, point 1b, one can observe in Fig. 5(c) that the field is concentrated in the region under the lamellae openings and rapidly decreases between them. In contrast, curve 3 of Fig. 4 presents a completely different field behavior. Figures 6(a)–6(d) give the field map distribution for the several different points of curve 3 with a gradual in-

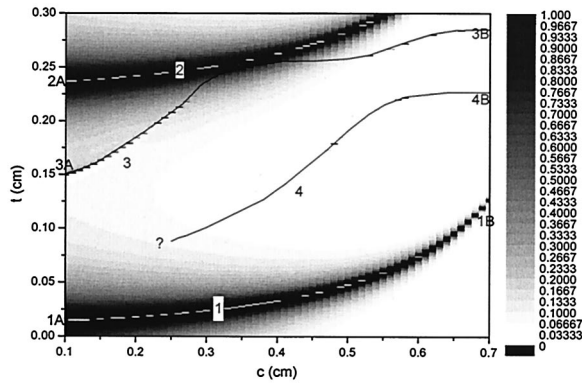


Fig. 7. Transmission as a function of the lamellae width (c) and middle-layer thickness (t) in centimeters for the grating represented in Fig. 3(b).

crease of the lamellae width. Figure 6(a), corresponding to point 3a of curve 3, exhibits three maxima along x and a single maximum along y . As already mentioned, this point corresponds to a waveguide-mode excitation that uses the first diffraction order of the grating. As far as the incidence is normal, simultaneous excitation of modes propagating in opposite directions of the x axis occurs, and the field distribution corresponds to a standing wave along x . When the lamellae width c is increased, the field distribution remains qualitatively the same (standing wave in the x direction); however, in contrast to Fig. 5, the field intensity between the metallic lamellae remains high, reflecting the fact that the enhanced resonant transmission is due to excitation of waveguide modes propagating in the $\pm x$ direction. As the groove opening reduces gradually [see Fig. 6(d)], the dielectric waveguide mode is gradually transformed into a mode of the corresponding metallic waveguide filled with the dielectric. The corresponding spectral and angular dependencies of the transmission will be analyzed later when a comparison is done with the cavity resonances.

Second, to observe the differences and similarities between waveguide and cavity modes, we analyze the structure presented in Fig. 3(b), which will be called the grating-cavity configuration. The difference with the previous case is the existence of a vertical metallic wall 0.1 cm thick, which serves to isolate the field inside the adjacent periods. This prohibits waveguide-mode propagation but permits the existence of new types of resonance, namely, cavity resonances.

The transmission of the structure as a function of the lamellae width and the cavity (filled with the same dielectric) height is presented in Fig. 7. Similar to Fig. 4, several well-distinguished regions can be observed, with the transmission reaching 100% along four curves. Some of these regions are wider in their t dependence (curves 1 and 2), whereas curves 3 and 4 are rather thin, so thin that it is impossible to follow curve 4 for values of c less than 0.25. The starting lamellae width is 0.1 cm because

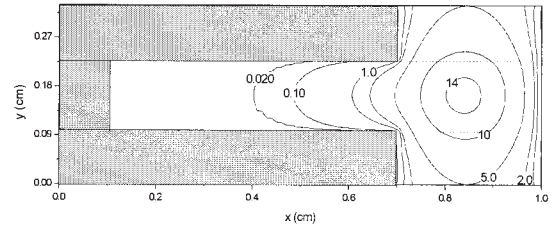


Fig. 8. Electric field maps corresponding to the working point 1B of Fig. 7.

this is the thickness of the walls that separate the grooves.

The similarities between the transmission behaviors for open- and close-groove gratings observed when we compare Fig. 4 with Fig. 7 are not accidental. Curves 1 and 2 in the two figures are due to Fabry-Perot resonances, presenting maxima in the y direction and having weak dependence in the x direction for narrow lamellae. Thus results not reported here have shown the same field distributions for points 1A and 2A of Fig. 7 as those reported in Figs. 5(a) and 5(b). The same conclusion is valid at the other end (c large, point 1B) of curve 1 of Fig. 7. Comparing Fig. 5(c) with Fig. 8, we see that the behavior of the field distribution remains the same as that of point 1b of Fig. 4.

Although the grating-cavity configuration under study [Fig. 3(b)] does not allow waveguide modes to propagate, in contrast to the system presented in Fig. 3(a), there exists for the grating-cavity configuration field distributions that allow for 100% resonant transmission, similar to the waveguide-mode excitation allowed in the system shown in Fig. 3(a). This phenomenon can be observed along curves 3 and 4 of Fig. 7. Figure 9 presents the electric field maps for the three points 3A, 3B, and 4B, which are quite similar to the field distributions presented in Figs. 6(a)-6(c). However, the main difference is that in Fig. 9 we observe the excitation of cavity resonances, a cavity formed by the vertical and horizontal metallic walls. The similarity with Fig. 6 is due to the fact that the waveguide modes are excited in normal incidence and thus present a standing-wave behavior similar to the cavity modes.

Increasing the horizontal lamellae width, one can observe a gradual transition between a resonator open in the vertical direction [Fig. 9(a)] to an almost closed resonator inside the cavity [Fig. 9(c)]. Although the field distribution along curve 3 of Fig. 4 and curves 3 and 4 of Fig. 7 are quite similar, as well as their dependence on the lamellae width c and the dielectric region thickness t , the angular and spectral behaviors could be quite different in the two cases, as well as when compared with the Fabry-Perot resonances. This is analyzed in what follows in the current section.

When the left-hand side of curves 1 and 2 in both Figs. 4 and 7 are considered, the enhanced transmission is due to Fabry-Perot resonances in (almost) open resonators. These are characterized by rela-

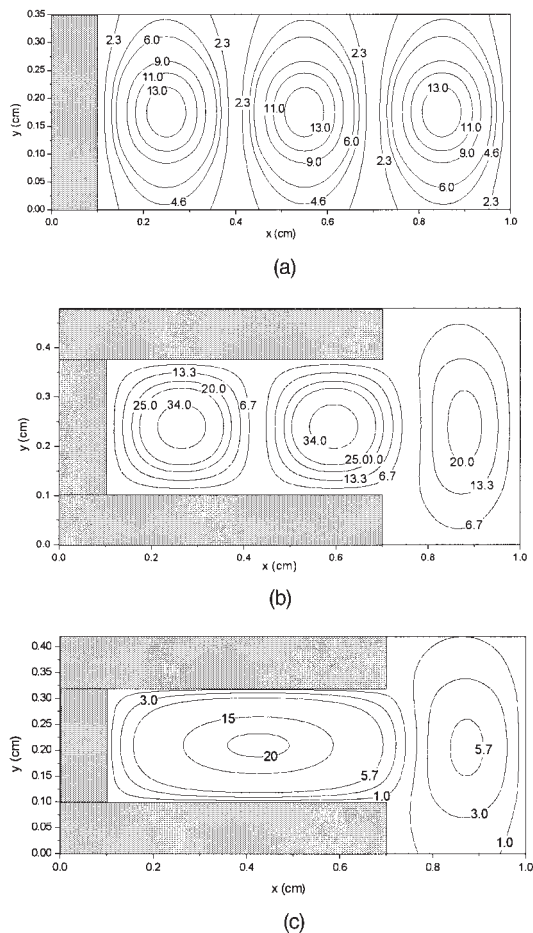


Fig. 9. Electric field maps corresponding to different working points along curves 3 and 4 of Fig. 7: (a) point 3A, (b) point 3B, and (c) point 4B.

tively large spectral and angular dependences. When the groove opening is reduced (increasing c), the resonator becomes more closed. How does this influence the spectral transmission curve? Figure 10(a) shows the spectral variation of the transmission in that case, with a spectral width at a half-height for both working points 1b and 1B of the order of 0.02 cm ($\Delta\lambda/\lambda = 1.3 \times 10^{-2}$), which is quite large; when compared further with the waveguide or cavity-mode excitation, it will be shown that closing the resonator reduces the spectral bandwidth. Anyway, the angular response for the Fabry–Perot resonance remains almost insensitive with respect to the incident angle, at least in the region in which only the specular orders of the grating propagate [Fig. 10(b)] (angle < 30 deg).

This behavior has to be compared with the waveguide-mode excitation process for the same lamellae width, presented in Fig. 11 for the working point 3d. The spectral width of the transmission maximum [Fig. 11(a)] is less than 0.0005 cm ($\Delta\lambda/\lambda = 3.10^{-4}$). The angular curve is also quite narrow [Fig. 11(b)], reflecting the fact that the waveguide mode is excited through the ± 1 st diffraction orders of the gratings; i.e., the resonant incident angle θ_i is

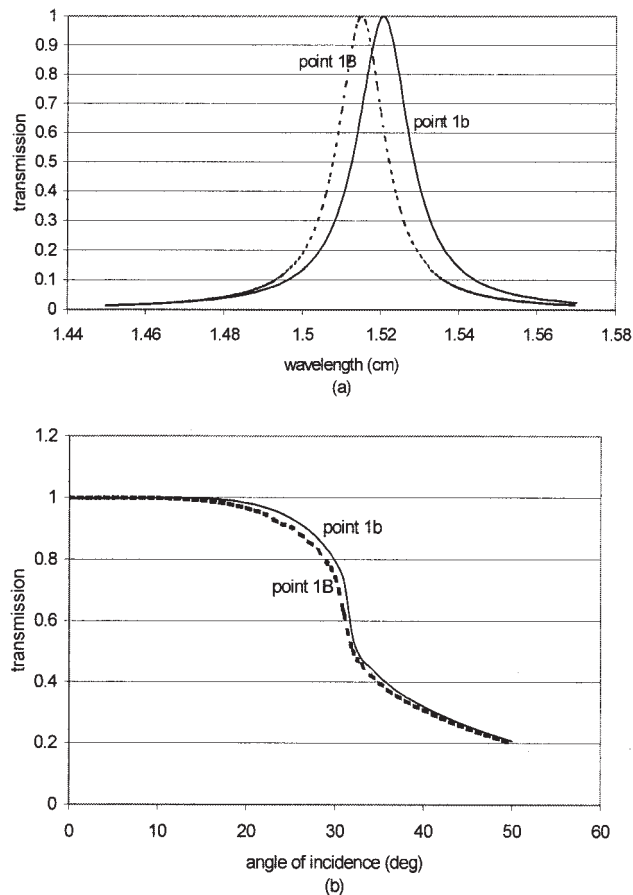


Fig. 10. Transmission corresponding to working points 1b of Fig. 4 and 1B of Fig. 7: (a) as a function of the wavelength and (b) as a function of the angle of incidence.

linked to the waveguide-mode propagation constant in the x direction γ_g by the grating equation

$$\sin \theta_i = \gamma_g \frac{\lambda}{2\pi} \pm \frac{\lambda}{d}. \quad (5)$$

The narrower the resonance in λ , the narrower in θ_i , which creates great problems for using the resonant waveguide-mode excitation for spectral filtering: Narrow filters require well-collimated incident light, a requirement that is quite often difficult to meet.

Cavity resonances could provide a simple solution to this problem. Closing the cavity by decreasing the opening will reduce the coupling with the incident light and will increase the finesse in λ and thus will diminish the width of the spectral maximum to a desired value. However, in contrast to what happens during the waveguide-mode excitation, in which the angular dependence also depends on the spectral width through Eq. (5), the cavity resonance could be quite thin in λ and quite large in θ_i . This can be understood by taking account of the fact that the cavity resonance depends on the optogeometrical parameters (cavity dimensions, optical index, and wavelength) so that the angle of incidence plays a much smaller role because its variation changes only

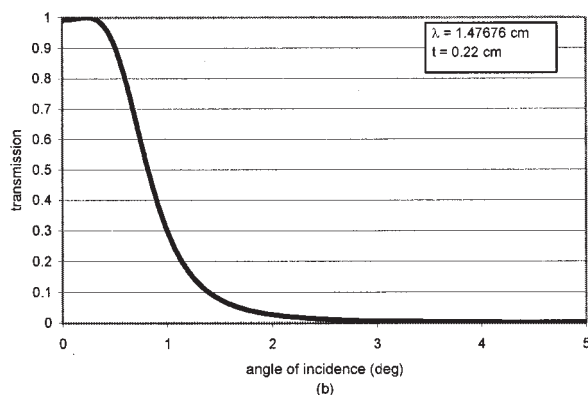
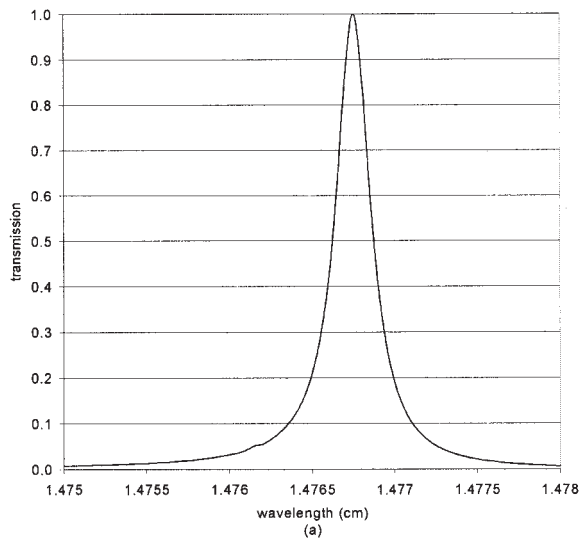


Fig. 11. Transmission corresponding to the working point 3d of Fig. 4: (a) as a function of the wavelength and (b) as a function of the angle of incidence.

the strength of resonance excitation and not the resonance characteristics themselves. And, indeed, under conditions similar to those of Fig. 11, Fig. 12 presents the spectral and angular dependences of the transmission close to the working point 4B of Fig. 7, i.e., for a closed resonance. As can be observed, using excitation of cavity resonances instead of waveguide modes, one can preserve a very narrow spectral resonance [$\Delta\lambda/\lambda \approx 3.10^{-4}$ in Fig. 12(a)] while preserving the spectral position of the maximum within a large angular interval [Fig. 12(b)]. Although the system is asymmetrical with respect to the vertical $y-z$ plane [see Fig. 3(b)], the angular dependence is almost symmetrical with respect to the normal incidence because the field map inside the cavity is also almost symmetrical [see Fig. 9(c)].

Another proof that cavity resonances are mainly guided by the cavity dimensions and not by the excitation conditions, in contrast to the waveguide-mode excitation governed by Eq. (5), is presented in Fig. 13, in which the spectral response close to working points 4B [Fig. 13(b)] and 3b [Fig. 13(c)] is analyzed when the groove period is increased while the cavity dimensions are preserved [Fig. 13(a)]. An increase of 10%

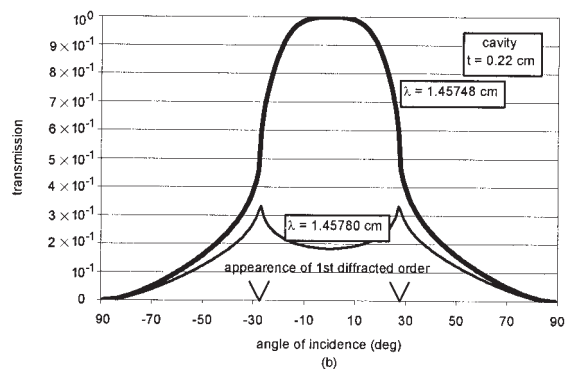
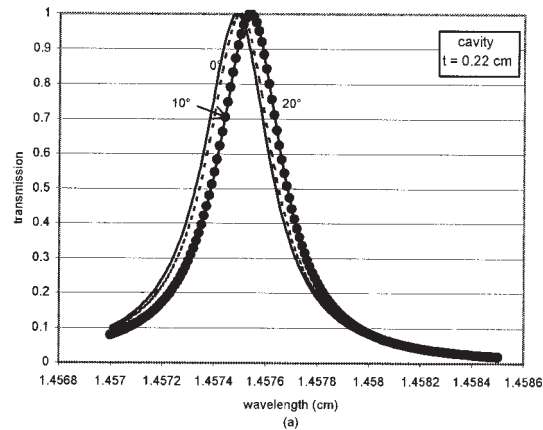


Fig. 12. Spectral (12a) and angular (12b) dependences of transmission at the working point 4B of Fig. 7.

of the period does not significantly modify the spectral response of the cavity resonance [Fig. 13(b)], whereas only a 1% change of the period when a waveguide mode is excited through Eq. (5) leads to a significant shift of the peak location in the spectral domain [Fig. 13(c)].

3. Two-Dimensional Grating

The aim of this section is to show how the ideas developed in Section 2 in the simpler case of one-dimensional gratings can be extended to two-dimensional gratings in order to suppress the sensitivity to the polarization of the incident light. Two kinds of grating will be considered: the woodpile structure and the square-grid grating.

The first one is the so-called woodpile structure, well known as being one of the most promising structures for building photonic crystals.¹⁹ Figure 14 depicts the four-layer woodpile structure; the parameters are given in the figure caption. In this case it can be proved that the transmission is insensitive to the polarization by use of the reciprocity theorem and symmetry. Indeed, let us consider the incident field corresponding to case (a) in Fig. 14.

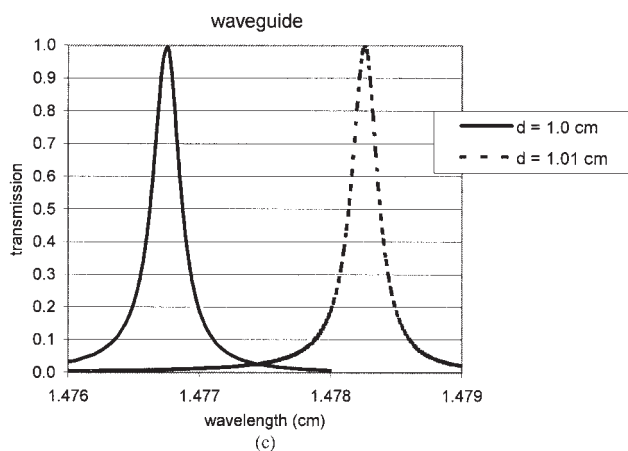
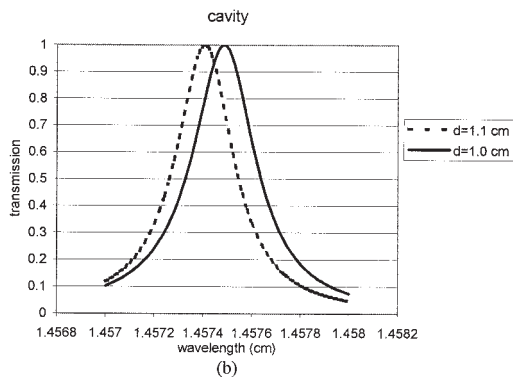
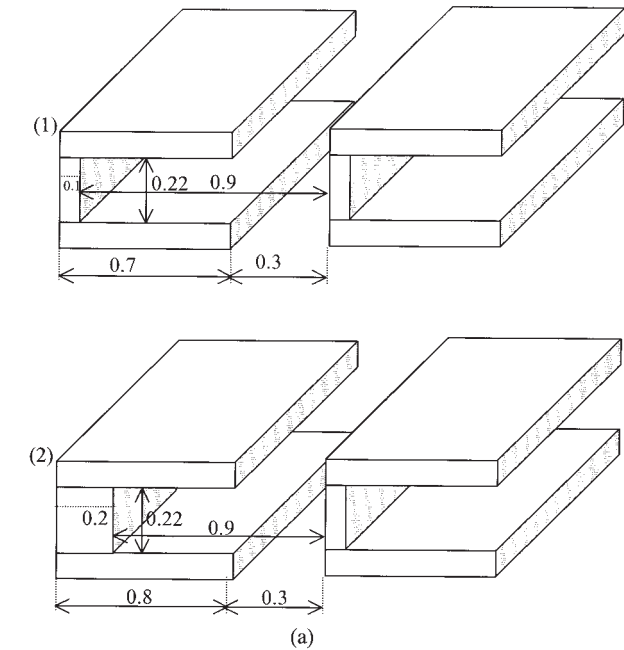


Fig. 13. Comparison of the influence of the period between the cavity modes and the waveguide modes. (a) Schematic representations of the cavity-type grating. (b) Influence of the period d of the cavity-type grating on the transmission as a function of the wavelength. (c) Influence of the period d of the one-dimensional double grating on the transmission as a function of the wavelength.

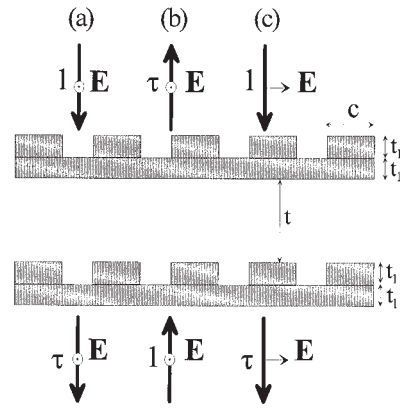


Fig. 14. Schematic representation of the woodpile gratings. The parameters are period $d = 1$ cm, $c = 0.7$ cm, $t = 0.715$ cm, $t_1 = 0.1$ cm, the optical index of the metal is $n_m = i 10^4$, and the structure is lying in vacuum.

The bold arrow represents the wave vector, and the electric field direction is orthogonal to the figure. If the amplitude of the incident field is normalized, let us call τ the amplitude of the transmitted field. From the reciprocity theorem²⁰ we know that if the incident field corresponds to case (b) the transmission will be the same (τ). Then, from the symmetry of the structure, it appears that an incident field with the electric field orthogonal to the figure and coming from the bottom [case (b)] is identical to an incident field with the electric field in the plane of the figure coming from the top [case (c)], and thus cases (a) and (c) must also be identical.

The structure is modeled by use of the rigorous modal method.²¹ In this method the field is expressed on the basis of the modes of the lamellar structure. Figure 15 shows the transmission as a function of the wavelength when the structure is illuminated by a plane wave in normal incidence and the electric field is normal to the plane of Fig. 14 (case a) or the electric field is in the plane of Fig. 14 (case b). As expected, the transmission presents a sharp peak that is the same for both cases. The physical origin of the peak is a Fabry-Perot resonance of the structure, each pair of crossed gratings acting as a mirror. Indeed, because the medium between the "mirrors" is vacuum, the higher propagation constant allowed for the excited mode is $k_0 = \omega/c$. Because the period is smaller than the wavelength, only the zero

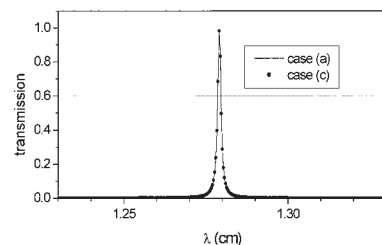


Fig. 15. Transmission of the woodpile grating of Fig. 14 in normal incidence.

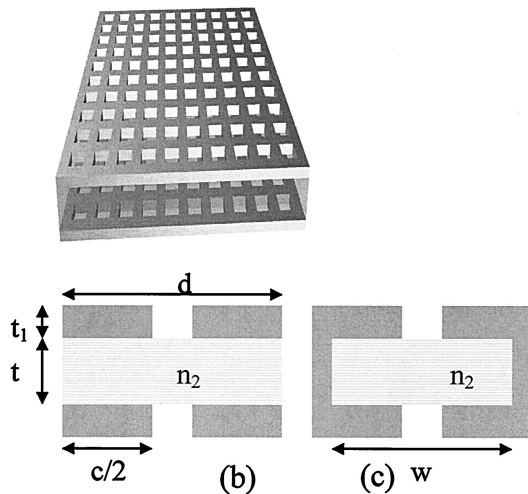


Fig. 16. Schematic representation of the biperiodic gratings. (a) Perspective view of the double grating with a continuous dielectric layer in the middle. (b) Section of the unit cell (along any of the periodicity axes) of the double grating with a continuous dielectric layer in the middle (slab type). (c) Section of the unit cell (along any of the periodicity axes) of the cavity-type grating. The parameters are $d = 1$ cm, $c = 0.5$ cm, $t = 0.22$ cm, $t_1 = 0.1$ cm, $w = 0.9$ cm, $n_2 = 3.47$, the optical index of the metal is $n_m = i 250$, and the structure is lying in vacuum.

order of the grating is propagative. Then the excited mode can have only a null tangential component of the wave vector (i.e., the Fabry–Perot mode in normal incidence).

The second structure is made of a dielectric slab placed between two metallic grids (square holes on a square lattice made in a metallic layer) as represented on Fig. 16(b) (slab-type grating). Figure 16(c) shows a variant of the structure: In the slab, vertical metallic walls are added to form cavities (cavity-type grating). Both structures are symmetric with respect to top-down symmetry; thus a transmission equal to 1 is expected for a lossless structure,¹⁵ whereas the x - y symmetry ensures a transmission insensitive to the polarization of the incident light. The metallic grid structures are modeled by use of the Fourier modal method.²² In the numerical code the modes are expressed on a Fourier basis, and both the fast Fourier factorization^{23,24} (the proper way to write products of truncated Fourier series) and the S-matrix algorithm²⁵ (to avoid numerical instabilities owing to growing exponentials) are used. Figure 17 shows the transmission in normal incidence of the slab-type grating as a function of the wavelength. The peak with maximum equal to 1 is due to the excitation of a guided mode of the slab as explained for the one-dimensional gratings in the previous sections; the mode is excited by the (1, 0) or (0, 1) order of the two-dimensional grating. Note that diminishing the size of the square holes of the grids can narrow the peak. All the parameters of the structure are given in the figure caption of Fig. 16.

Figure 18 shows the transmission in normal incidence for the cavity-type grating as a function of the

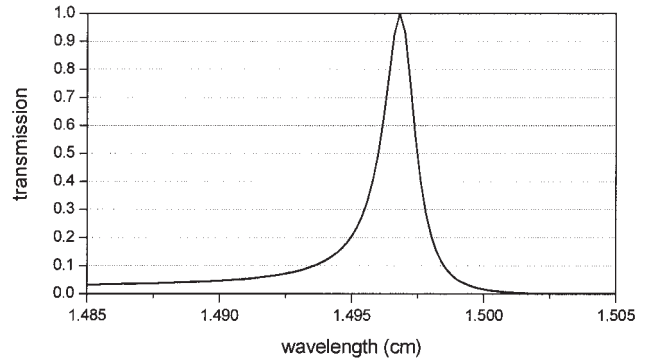


Fig. 17. Transmission of the slab-type grating [Fig. 16(b)] in normal incidence.

wavelength. When compared with Fig. 17, Fig. 18 does not differ notably. The value of the maximum of the peak has slightly changed, and the width of the peak is similar. Figure 19 shows the transmission for both structures as a function of the angle of incidence for the wavelength corresponding to the maximum value of the transmittance in Figs. 17 and 18 (for the slab-type grating and the cavity-type grating, respectively). The remarkable result is that the transmission of the cavity-type grating remains very high on the whole range of angle of the figure (20 deg),

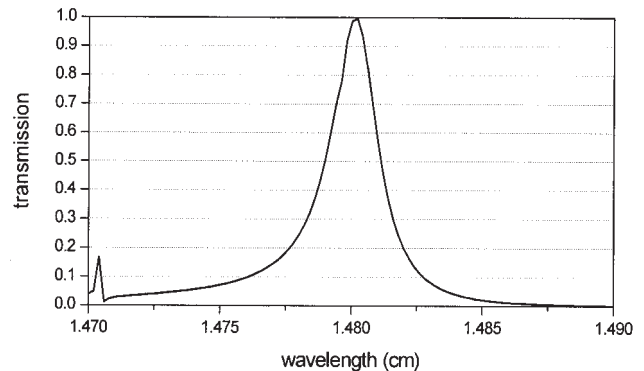


Fig. 18. Transmission of the cavity-type grating [Fig. 16(c)] in normal incidence.

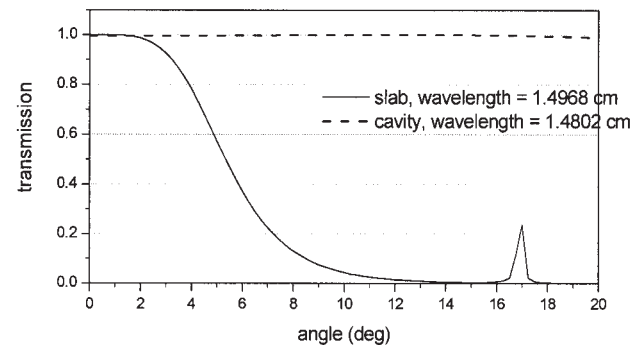


Fig. 19. Transmission of the slab-type grating [Fig. 16(b)] for $\lambda = 1.4968$ cm (solid curve) and of the cavity-type grating [Fig. 16(c)] for $\lambda = 1.4802$ cm (dashed curve).

whereas the transmission of the slab-type grating falls to approximately 0.5 for an angle of only 5 deg. This result confirms the demonstration made in Section 2 on the one-dimensional grating.

4. Conclusion

The enhanced transmission through subwavelength grids or hole arrays observed by Ebbesen *et al.*⁵ in the visible region and linked with the resonant excitation of surface plasmons can be obtained in spectral domains and for polarizations for which plasmons are lacking or inoperative. The high transmission is then linked with the excitation of other electromagnetic resonances among which are Fabry–Perot, waveguide-mode, and cavity-mode resonances. The first type produces transmission curves with large spectral and angular bandwidths, compared with waveguide-mode resonances, whereas cavity-resonance excitation can achieve simultaneously high finesse in λ and large bandwidth in incidence, as well a spectral peak location almost independent of the grating period. These characteristics are common to both one-dimensional and two-dimensional gratings. They can be of great interest in realizing nanosources for the far-infrared and microwave domains. From a theoretical point of view, it is simple to extend the validity of our results to the visible domain. As far as the refractive indices are kept unchanged, rescaling all dimensions by a factor of 10^{-4} moves the wavelength from 1 cm to 1 μm . However, from the experimental point of view, it is impossible to find materials with optical indices used in this study at wavelengths of the order of 1 μm . On the other hand, in the visible domain, the plasmon resonances can play a significant role in enhancing the transmission.

It is necessary to point out that the present study addresses configurations having periodicity in one (gratings) or two dimensions (arrayed holes and crossed gratings) and does not concern enhanced transmission through single (patterned or not) holes.

The research of B. Gralak is part of the research program of the Foundation for Fundamental Research on Matter and was made possible by financial support from the Dutch Foundation of Scientific Research.

References

1. R. Wood, "On a remarkable case of uneven distribution of light in a diffraction grating spectrum," *Philos. Mag.* **4**, 396–402 (1902).
2. U. Fano, "The theory of anomalous diffraction gratings and of quasi-stationary waves on metallic surfaces (Sommerfeld's waves)," *J. Opt. Soc. Am.* **31**, 213–222 (1941).
3. H. Kogelnik, "Theory of dielectric waveguides," in *Integrated Optics*, T. Tamir, ed. (Springer, Berlin, 1975), Chap. 2.
4. L. Mashev and E. Popov, "Zero order anomaly of dielectric coated grating," *Opt. Commun.* **55**, 377–380 (1985).
5. T. W. Ebbesen, H. J. Lezec, H. F. Ghaemi, T. Thio, and P. A. Wolff, "Extraordinary optical transmission through subwavelength hole arrays," *Nature* **391**, 667–669 (1998).
6. S. Enoch, E. Popov, M. Nevière, and R. Reinisch, "Enhanced light transmission by hole arrays," *J. Opt. A Pure Appl. Opt.* **4**, S83–S87 (2002).
7. N. Bonod, S. Enoch, L. Li, E. Popov, and M. Nevière, "Resonant optical transmission through thin metallic films with and without holes," *Opt. Express* **11**, 482–490 (2003), <http://www.opticsexpress.org>.
8. K. Knop, "Reflection grating polarizer for the infrared," *Opt. Commun.* **26**, 281–283 (1978).
9. Z. Bomzon, V. Kleiner, and E. Hasman, "Computer-generated space-variant polarization elements with subwavelength metal stripes," *Opt. Lett.* **26**, 33–35 (2001).
10. N. Bokor, R. Shechter, N. Davidson, A. Frieseman, and E. Hasman, "Achromatic phase retarder by slanted illumination of a dielectric grating with period comparable with the wavelength," *App. Opt.* **40**, 2076–2080 (2001).
11. A. P. Hibbins, J. R. Sambles, and C. R. Lawrence, "The coupling of microwave radiation to surface plasmon polaritons and guided modes via dielectric gratings," *J. Appl. Phys.* **87**, 2677–2683 (1999).
12. A. P. Hibbins, J. R. Sambles, C. R. Lawrence, and D. M. Robinson, "Remarkable transmission of microwaves through a wall of long metallic bricks," *Appl. Phys. Lett.* **79**, 2844–2846 (2001).
13. A. P. Hibbins, J. R. Sambles, and C. R. Lawrence, "Grating-coupled surface plasmons at microwave frequency," *J. Appl. Phys.* **86**, 1791–1795 (1999).
14. R. C. McPhedran, G. H. Derrick, and L. C. Botten, "Theory of crossed grating," in *Electromagnetic Theory of Gratings*, Vol. 22 of Topics in Current Physics, R. Petit, ed. (Springer-Verlag, Berlin, 1980), p. 249.
15. E. Popov, L. Mashev, and D. Maystre, "Theoretical study of the anomalies of coated dielectric gratings," *Opt. Acta* **33**, 607–619 (1986).
16. M. G. Moharam and T. K. Gaylord, "Rigorous coupled-wave analysis of metallic surface-relief gratings," *J. Opt. Soc. Am. A* **3**, 1780–1787 (1986).
17. I. C. Botten, M. S. Craig, R. C. McPhedran, J. L. Adams, and J. R. Andrewartha, "The finitely conducting lamellar diffraction grating," *Opt. Acta* **28**, 1087–1102 (1981).
18. R. Petit and G. Bouchitté, "Replacement of a very fine grating by a stratified layer, homogenization techniques, and multiple-scale method theory," in *Application and Theory of Periodic Structures, Diffraction Gratings, and Moiré Phenomena 431*, J. Lerner, ed., *Proc. SPIE* **815**, 25–31 (1988).
19. S. Y. Lin, J. G. Flemming, D. L. Hetherington, B. K. Smith, R. Biswas, K. M. Ho, M. M. Sigalas, W. Zubrzycki, S. R. Kurtz, and J. Bur, "A three-dimensional photonic crystal operating at infrared wavelength," *Nature* **394**, 251–253 (1998).
20. R. Petit, "A tutorial introduction," in *Electromagnetic Theory of Gratings*, Vol. 22 of Topics in Current Physics, R. Petit, ed. (Springer-Verlag, Berlin, 1980), p. 12.
21. B. Gralak, M. De Dood, G. Tayeb, S. Enoch, and D. Maystre, "Theoretical study of photonic bandgaps in woodpile crystals," *Phys. Rev. E* **67**, 066601 (2003).
22. L. Li, "New formulation of the Fourier modal method for crossed surface-relief gratings," *J. Opt. Soc. Am. A* **14**, 2758–2767 (1997).
23. E. Popov and M. Nevière, "Maxwell equations in Fourier space: fast converging formulation for diffraction by arbitrary shaped, periodic, anisotropic media," *J. Opt. Soc. Am. A* **18**, 2886–2894 (2001).
24. M. Nevière and E. Popov, *Light Propagation in Periodic Media: Differential Theory and Design* (Marcel Dekker, New York, 2003).
25. L. Li, "Formulation and comparison of two recursive matrix algorithms for modeling layered diffraction gratings," *J. Opt. Soc. Am. A* **13**, 1024–1035 (1996).